ACS APPLIED MATERIALS & INTERFACES

Research Article

www.acsami.org

Creating SERS Hot Spots on MoS_2 Nanosheets with in Situ Grown Gold Nanoparticles

Shao Su,[†] Chi Zhang,[†] Lihui Yuwen,[†] Jie Chao,*[,‡] Xiaolei Zuo,[‡] Xingfen Liu,[†] Chunyuan Song,[†] Chunhai Fan,[†,‡] and Lianhui Wang*[,†]

[†]Key Laboratory for Organic Electronics & Information Displays (KLOEID), Institute of Advanced Materials (IAM), and School of Materials Science and Engineering, Nanjing University of Posts & Telecommunications, 9 Wenyuan Road, Nanjing 210046, China

[‡]Division of Physical Biology, Shanghai Institute of Applied Physics, Chinese Academy of Sciences, Shanghai 201800, China

Supporting Information

ABSTRACT: Herein, a reliable surface-enhanced Raman scattering (SERS)-active substrate has been prepared by synthesizing gold nanoparticles (AuNPs)-decorated MoS_2 nanocomposite. The AuNPs grew in situ on the surface of MoS_2 nanosheet to form efficient SERS hot spots by a spontaneous redox reaction with tetrachloroauric acid ($HAuCl_4$) without any reducing agent. The morphologies of MoS_2 and AuNPs-decorated MoS_2 nanosheet were characterized by TEM, HRTEM, and AFM. The formation of hot spots greatly depended on the ratio of MoS_2 and $HAuCl_4$. When the concentration of $HAuCl_4$ was 2.4 mM, the as-prepared AuNPs@MoS_2-3 nanocomposite exhibited a high-quality SERS activity toward probe molecule due to the generated hot spots. The spot-to-spot SERS signals showed that the relative standard deviation (RSD) in the intensity of the main Raman vibration modes (1362, 1511, and 1652 cm^{-1}) of Rhodamine 6G were about 20%, which displayed good uniformity and reproducibility. The AuNPs@MoS_2-based substrate was reliable, sensitive, and reproducible, which showed great potential to be an excellent SERS substrate for biological and chemical detection.

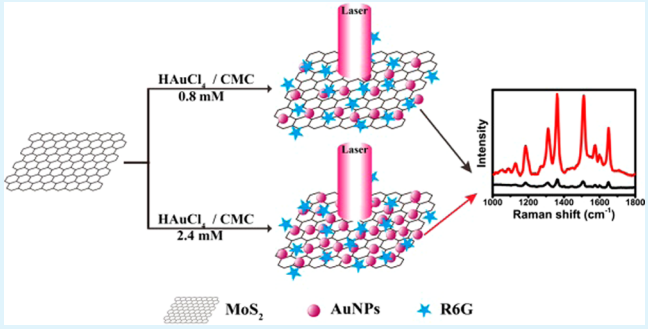

KEYWORDS: *AuNPs@MoS_2 nanocomposite, SERS-active substrate, hot spot, uniformity*

INTRODUCTION

Surface-enhanced Raman scattering (SERS) is one of the most powerful and ultrasensitive analytical technique in biosensors,[1,2] biological imaging[3] and environmental monitoring[4] due to its unique vibrational fingerprints of the analytes.[5] Furthermore, the SERS signals can be amplified to 10^{12}–10^{15} times when the target molecules reside on the proper position between metal nanostructures (generally called "hot spots"), enabling the possibility of single-molecule detection.[5] In general, hot spots are not only formed by noble metal nanoparticles (Au, Ag and Cu),[6] but also generate from metal nanoparticles and metal surfaces.[7] Therefore, metal nanostructures decorated on the surface of SERS-active substrates generated SERS signal amplification effect, which has gradually attracted greatly attentions.[8] Interestingly, it has been found that molybdenum disulfide (MoS_2) can generate weak SERS activity.[9] To obtain better SERS effect, increasingly more researchers have focused on functionalizing the nanomaterials to construct better SERS-active substrate for SERS applications. For example, Zhao et al. fabricated AgNPs-decorated MoS_2 nanosheet for 2-mercapto-benzimidazole detection according to a wet chemistry procedure.[10] Zhan and co-worker observed an improved Raman enhancement of R6G molecules deposited on oxygen−plasma MoS_2 and argon−plasma treated MoS_2 nanoflakes.[11] Although many SERS-active nanocomposite substrates have been reported, constructing efficient SERS-active platforms is still a challenge for ultrahigh and reproducible detection.

MoS_2 is a typical layered two-dimensional (2D) chalcogenide material, which has attracted increasing interest for its novel nanoelectronic and optoelectronic properties.[12] As a graphene analogue, MoS_2 nanosheet has distinct similarities compared to graphene such as 2D ultrathin atomic layer structure and high surface area, which shows a great potential in nanoelectronics, optoelectronics, and energy harvesting.[13,14] Furthermore, MoS_2 is considered as a promising supporting material to stabilize metal nanoparticles (NPs), forming hierarchical composites. As we know, noble metal nanoparticles such as Au, Pt and Ag are broadly used in biosensing, photonics and catalysis because of their unique chemical and physical properties. Therefore, it can be expected that the noble metal nanoparticles (NPs) decorated on the MoS_2 sheet could potentially extend its

Received: July 2, 2014
Accepted: October 13, 2014
Published: October 13, 2014

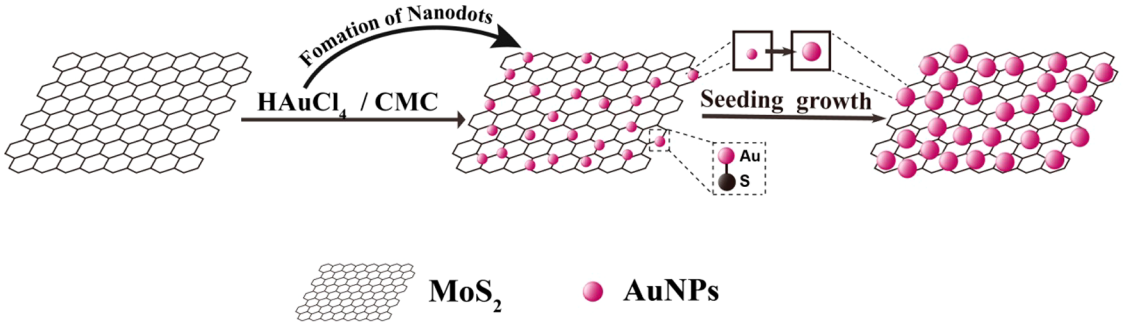

Figure 1. Schematic illustration of synthesizing AuNPs@MoS_2 nanocomposite.

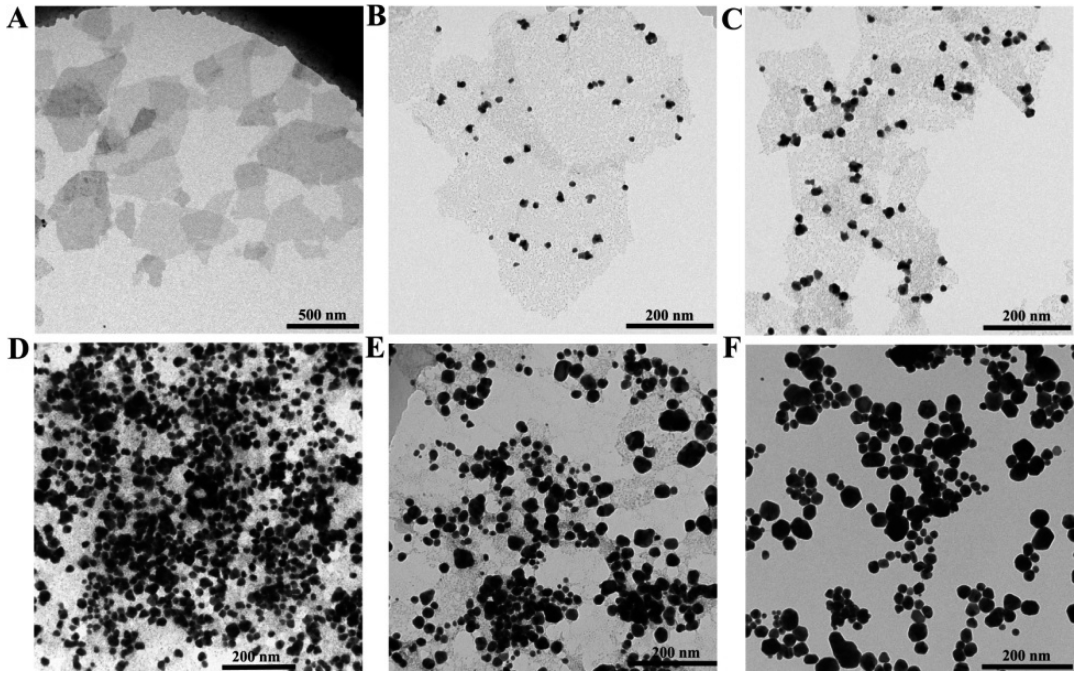

Figure 2. TEM images of (A) MoS_2, (B) AuNPs@MoS_2-1, (C) AuNPs@MoS_2-2, (D) AuNPs@MoS_2-3, (E) AuNPs@MoS_2-4, and (F) AuNPs@MoS_2-5.

functionalities as novel catalytic, magnetic, and optoelectronic nanomaterials. Up to now, a few reports have focused on the preparation of noble metal nanoparticles@MoS_2 nanocomposites. For example, Zhang's group employed the solution-processable MoS_2 nanosheets to direct the epitaxial growth of Pd, Pt and Ag nanostructures at ambient conditions.[15] Shi et al. found that gold nanoparticles (AuNPs) could be selectively formed on the edge sites or defective sites of MoS_2 nanosheets.[16] Huang's group had reported that AuNPs@MoS_2 could significantly enhance electrocatalytic performance toward hydrogen evolution reactions.[17] Our group also had proved that noble metal nanoparticles could efficiently decorated on the surface of MoS_2 nanosheet by chemical synthesis and electrodeposition technique.[18,19] Unfortunately, many synthetic strategies required the reduction agent to assist AuNPs grown in situ on MoS_2 nanosheet, such as trisodium citrate,[15] ascorbic acid[18] and hydroxyl amine.[20]

Herein, a facile and green method has been developed to construct SERS-active substrate by in situ growing AuNPs on MoS_2 nanosheet's surface. The MoS_2 nanosheet directly reacted with gold precursor ($HAuCl_4$) without any reduced agents by taking use of carboxymethyl cellulose (CMC) as stabilizer in aqueous solution. Because MoS_2 compounds have shown great ability in redox chemistry, they could directly react with metal precursors to allow a straightforward and green synthesis of AuNPs-decorated MoS_2 nanosheets (illustrated as Figure 1). Interestingly, the character of the AuNPs-loaded MoS_2 surface was changed with altering the concentration of $HAuCl_4$. The as-prepared MoS_2-based substrate possessed synergistic effects of the intrinsic properties of the AuNPs and MoS_2, making the AuNPs@MoS_2 nanocomposites exhibit attractive SERS application. More importantly, the AuNPs@MoS_2-3 nanocomposite generated more hot spots and obvious synergistic effect, which exhibited higher SERS activity toward the probe molecules than AuNPs@MoS_2-4 and AuNPs@MoS_2-5 nanocomposites.

EXPERIMENTAL SECTION

Reagents and Materials. *N*-Butyllithium (*n*-BuLi, 2.4 M hexane solution) was bought from Amethyst. Rhodamine 6G (R6G), gold(III) tetrachloride trihydrate ($HAuCl_4 \cdot 3H_2O$, ≥47.8%), sodium carboxymethyl cellulose (CMC, 800−1200 mPa·s), and molybdenum(IV) sulfide powder (<2 μm, 99%) were purchased from Sigma and used without further purification. All chemicals were directly used without further purification. All solutions were prepared with Milli-Q water from a Milli-pore system.

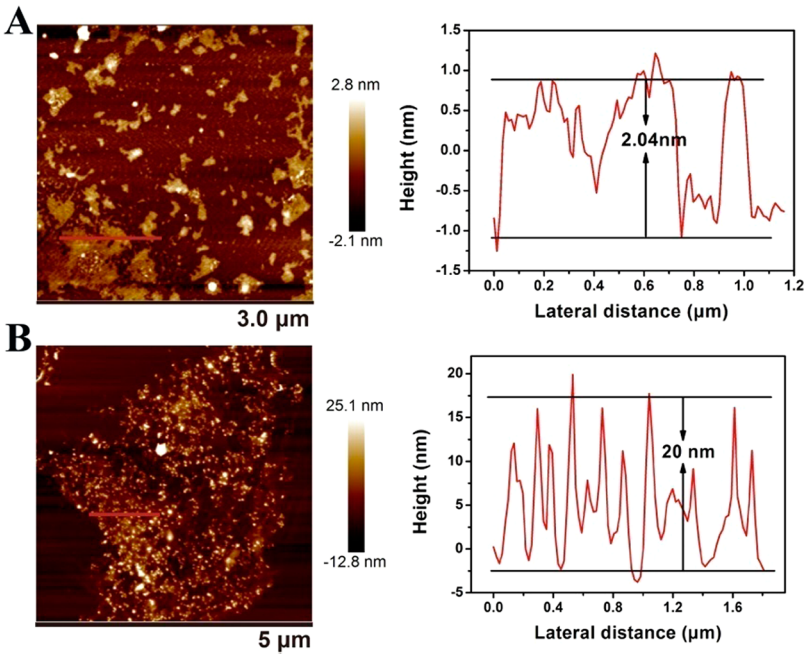

Figure 3. AFM images of (A) MoS_2 and (B) AuNPs@MoS_2-3 nanocomposite.

Apparatus and Measurements. UV−vis-NIR adsorption spectra were measured on a Shimadzu UV-3600 spectrophotometer. Transmission electron microscope (TEM) images were taken on a Hitachi H-7500 electron microscope (120 kV), and high-resolution TEM (HRTEM) characterization was performed on a Philips CM 200 electron microscope (200 kV) equipped with an energy dispersive X-ray spectrometer (EDS). Surface morphologies of MoS_2 nanosheet and the selected AuNPs@MoS_2 nanocomposite were examined with atomic force microscope (AFM, Bruker). The SERS analysis was performed on a HR800 Raman microscope instrument produced by HORIBA Jobin Yvon (France). The instrument is equipped with a standard 632.8 nm HeNe 20 mW laser. SERS experimental condition: $\lambda_{excitation}$ = 633 nm, acquisition time = 1 s, laser power = 20 mW, hole = 1000, slit = 100, grating = 600, and filter = D2.

Preparation of MoS_2 and AuNPs@MoS_2 Nanocomposite. MoS_2 nanosheets were prepared using the intercalation-exfoliation method developed by Joensen with some modifications.[21] Under Ar atmosphere, 0.3 g MoS_2 was intercalated with 10 mL of *n*-butyllithium solution at room temperature for 2 days. The unreacted *n*-butyllithium solution was removed and the residual solvent was removed by Ar gas flow. Oxygen-free water was added to exfoliate the Li intercalated MoS_2, and then the suspension was sonicated for 1 h to assist the exfoliation process. Finally, the aqueous dispersion of MoS_2 nanosheets was centrifuged at least twice to remove the LiOH and other soluble impurities.

AuNPs-decorated MoS_2 nanocomposite was synthesized by microwave-assisted hydrothermal method. In a typical synthesis, 5 mL (0.08 mg/mL) of MoS_2 nanosheets aqueous dispersion was added into a 10 mL quartz tube equipped with a magnetic bar. Under vigorous stirring, 400 μL of CMC (50 mM) and different aliquots of 100 mM $HAuCl_4 \cdot 3H_2O$ were immediately mixed with MoS_2 nanosheets solution. Then, the reaction mixture was heated to 60 °C for 5 min in the microwave reactor. Finally, the product of AuNPs@MoS_2 nanocomposite was purified by centrifugation.

RESULTS AND DISCUSSION

The morphologies of MoS_2 and AuNPs-decorated MoS_2 nanosheets were characterized by TEM and HRTEM. Figure 2A showed the typical TEM image of MoS_2 nanosheets, indicating that these nanosheets were not monolayer. To determine the layers, AFM was employed to examine the thickness of these MoS_2 nanosheets. As observed from the AFM image, the average height of MoS_2 nanosheets was about 2.0 nm (Figure 3A), suggesting that the prepared MoS_2 nanosheets were dilayer.[22,23] It has been reported that MoS_2/$AuCl_4^-$ should form a redox pair, allowing spontaneous reduction of gold ions to gold nanoparticles in situ on the MoS_2 nanosheets.[17] To prove the MoS_2 nanosheets can be used as reducing agent, the MoS_2 nanosheets and $HAuCl_4$ solution were mixed without adding any reducing agents. The MoS_2 nanosheets decorated with AuNPs were examined by changing the amount of $HAuCl_4$ and keeping other conditions unaltered. Interestingly, the morphology of AuNPs@MoS_2 nanocomposite could be tuned by different amount of $HAuCl_4$. As shown in Figure 2B−F, the size of AuNPs and the aggregation of AuNPs were changed with the concentration of $HAuCl_4$ from 0.8 to 4 mM. Only few and small AuNPs were dispersed on the MoS_2 nanosheets with 0.8 mM $HAuCl_4$ addition (AuNPs@MoS_2-1, Figure 2B). When the concentration of $HAuCl_4$ was increasing, the AuNPs grew larger and became aggregated (AuNPs@MoS_2-2, Figure 2C). As the concentration of $HAuCl_4$ is 2.4 mM, a uniform, high-density AuNPs-decorated MoS_2 nanocomposite was obtained (AuNPs@MoS_2-3, Figure 2D). However, the MoS_2 nanosheet began to be damaged when the $HAuCl_4$ concentration was up to 3.2 mM (AuNPs@MoS_2-4, Figure 2E). When the concentration of $HAuCl_4$ was 4 mM, the MoS_2 nanosheet almost disappeared, leaving only AuNPs aggregation (AuNPs@MoS_2-5, Figure 2F). This reason was that $HAuCl_4$ possessed high oxidation activity and continually reacted with MoS_2, resulting in Mo atoms that were oxidized to water-soluble, higher valence forms and leaching into the solution.[20] In conclusion, the density and size of the AuNPs decorating the MoS_2 nanosheets can be easily tuned by controlling the amount of $HAuCl_4$.

AFM was also employd to study the AuNPs@MoS_2 nanocomposite. Taking AuNPs@MoS_2-3 for example, Figure 3B clearly shows that AuNPs with a diameter around 20 nm were successfully decorated on the surface of MoS_2 nanosheet.

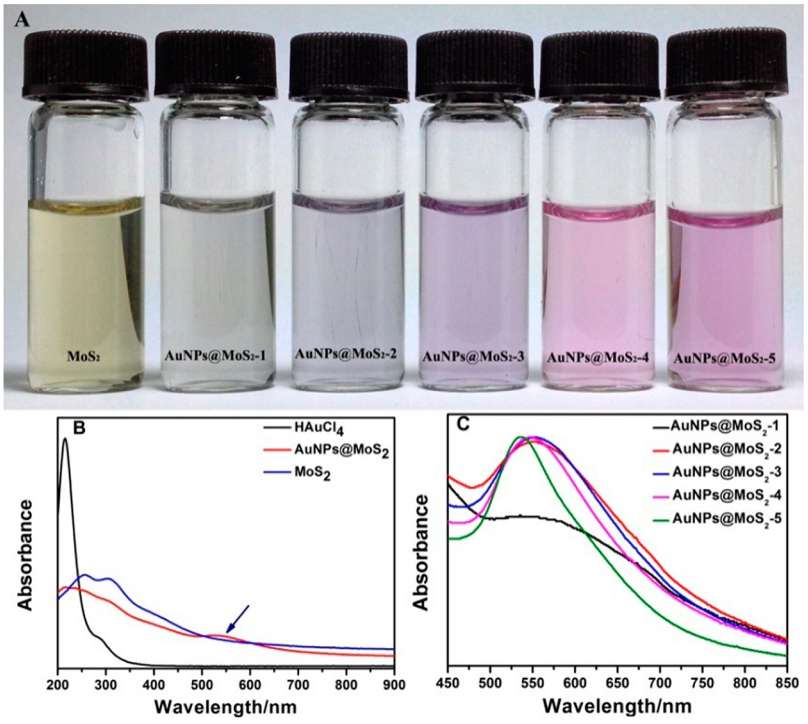

Figure 4. Spontaneous decoration of gold nanoparticles on MoS_2 nanosheets. (A) Photo images of MoS_2 nanosheets and different AuNPs@MoS_2 nanocomposite. (B) UV−vis spectra of MoS_2, $HAuCl_4$, and AuNPs@MoS_2 nanocomposite. (C) UV−vis spectra of different AuNPs@MoS_2 nanocomposite.

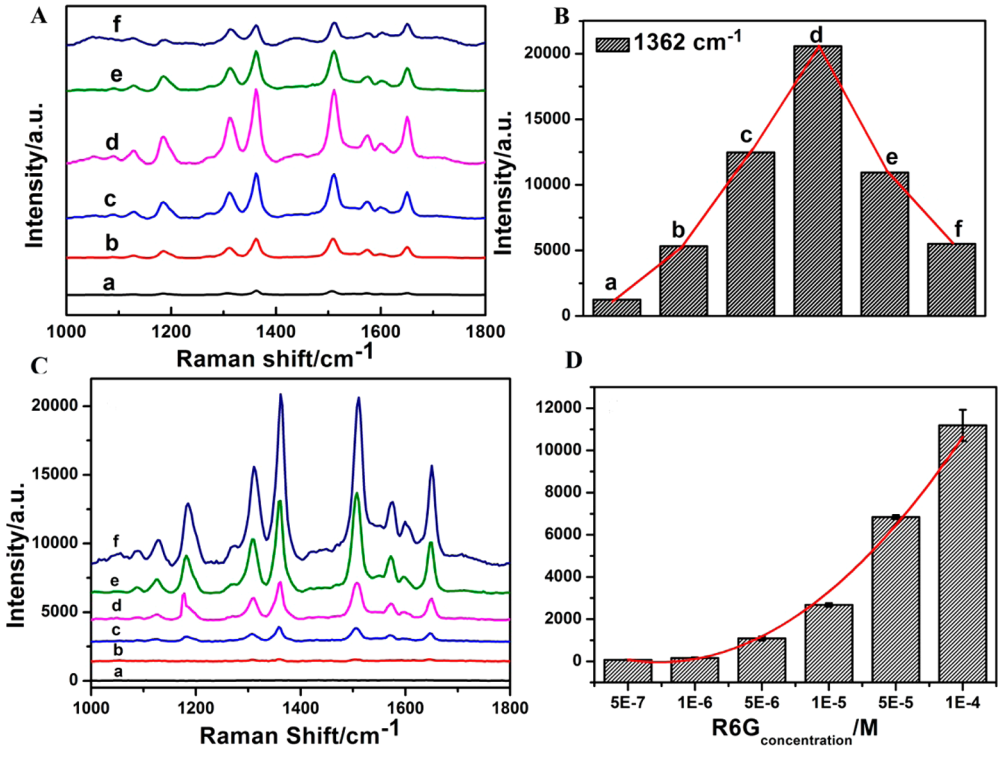

Figure 5. (A) SERS spectra of R6G molecules and (B) Raman intensity of R6G molecules collected on different SERS-active substrate: (a) MoS_2, (b) AuNPs@MoS_2-1, (c) AuNPs@MoS_2-2, (d) AuNPs@MoS_2-3, (e) AuNPs@MoS_2-4, and (f) AuNPs@MoS_2-5. (C) SERS spectra of R6G molecules with different concentrations (a) 5×10^{-7} M, (b) 10^{-6} M, (c) 5×10^{-6} M, (d) 10^{-5} M, (e) 5×10^{-5} M, and (f) 10^{-4} M. (D) Raman intensity of R6G at 1362 cm^{-1} for various R6G concentrations.

More interestingly, with the AuNPs decoration, the MoS_2 nanosheet gradually becomes a porous structure. The AFM image further proved that a small portion of Mo atoms may be oxidized to water-soluble, higher valence forms and leached into the solution, resulting in the MoS_2 nanosheet damaged. The HRTEM (Supporting Information Figure S1), EDX

spectroscopy (Supporting Information Figure S2) and Raman spectroscopy (Supporting Information Figure S3) were also used to prove that AuNPs had successfully decorated on the surface of MoS_2 nanosheet. From HRTEM image and the size distribution of AuNPs, the average of AuNPs in the AuNPs@MoS_2-3 nanocomposite was about 20 nm. After decoration of AuNPs on the MoS_2 nanosheet via microwave-assisted method, the Raman peaks of E^1_{2g} (378 cm^{-1}) and A_{1g} (401 cm^{-1}) showed a small blue shift and the Raman intensity greatly enhanced, suggesting the AuNPs had successfully decorated on the surface of MoS_2 nanosheet.

The AuNPs loaded on the surface of MoS_2 was also confirmed by the UV−vis spectra. As shown in Figure 4B, when a small aliquot of $HAuCl_4$ was added into chemically exfoliated MoS_2, the absorption peak of the gold precursor at around 215 nm significantly decreased. Meanwhile, a new absorption peak corresponding to the Au plasmon band at around 550 nm emerged, suggesting the consumption of Au^{3+} and the formation of gold nanoparticles. Upon mixing, an obvious color change was observed as the dispersion changed from yellow to purple and from purple to wine with the concentration of $HAuCl_4$ increasing (Figure 4A). The UV−vis spectra of AuNPs@MoS_2 hybrids would exhibit a red shift in the concentration of $HAuCl_4$ from 0.8 mM to 1.6 mM, indicating the size of formed AuNPs was increasing. Then, there is almost no red-shift between AuNPs@MoS_2-2 and AuNPs@MoS_2-3 (from 1.6 to 2.4 mM). As the concentration of $HAuCl_4$ over 3.2 mM, the AuNPs@MoS_2 hybrids exhibited narrower and a blue shift from 551 to 546 nm and 536 nm at 3.2 mM and 4 mM, respectively. As we know, the color of AuNPs changed with their diameter and UV−vis spectra.[24] In this experiment, the UV−vis spectra of AuNPs@MoS_2 nanocomposite was generated from the synergic effect of the AuNPs and MoS_2 nanosheets in solution. Therefore, the plasmon coupling and refractive index effects may originate the experimentally observed UV−vis band red-shift and broadening.

As mentioned above, MoS_2 nanosheets decorated with different density and size of AuNPs has been synthesized. To select the best SERS-active substrate, the standard probe (R6G) was employed to study the SERS performance of different AuNPs@MoS_2 nanocomposites. The strong Raman peaks at 1187, 1311, 1362, 1511, and 1652 cm^{-1} were in good agreement with previous reports of pure R6G or R6G on nanomaterials-based SERS substrate.[25,26] As shown in Figure 5A, MoS_2 nanosheets and AuNPs@MoS_2 nanocomposites possessed different Raman enhanced effect toward R6G molecule. Weak Raman signal of R6G was detected on MoS_2 nanosheets and AuNPs (Supporting Information Figure S4), while much stronger Raman signals of R6G were observed on AuNPs@MoS_2 nanocomposites. Moreover, the Raman intensity of R6G was increasing with the MoS_2 nanosheets decorated with more AuNPs. Unexpectedly, the Raman intensity of R6G on AuNPs@MoS_2-4 and AuNPs@MoS_2-5 nanocomposites was weaker than that on AuNPs@MoS_2-3 nanocomposite. As we know, Raman enhancement is caused by chemical enhancing mechanism and electromagnetic mechanism, depending on the compositions of SERS-active substrates. Recent reports showed that MoS_2 nanosheet could be used as a SERS substrate, which can absorb target molecules and a chemical enhancing mechanism for this SERS effect.[9,10] In addition, different size, density and aggregation of AuNPs would cause different SERS influences on the molecules, which were considered as well-known Raman substrates for chemical and biological detection. Therefore, the SERS effect of AuNPs@MoS_2 nanocomposite depends on the AuNPs size, density and MoS_2 nanosheet. From the TEM images, the aggregation of AuNPs was different in the AuNPs@MoS_2-3, -4, and -5. In the AuNPs@MoS_2-3, AuNPs have close to each other and a little aggregation, which can generate more hot spots than that seriously aggregated in the AuNPs@MoS_2-4 and AuNPs@MoS_2-5. The more hot spot there are, the stronger the SERS signal. Moreover, MoS_2 nanosheet has been damaged in the AuNPs@MoS_2-4 and almost disappeared in the AuNPs@MoS_2. As we know, the synergic effect is better that the single effect. Therefore, the SERS performance of AuNPs@MoS_2-3 was superior to AuNPs@MoS_2-4 and AuNPs@MoS_2-5 (Figure 5B), which was agreement with the previously reported work.[27] For the purpose of obtaining the high sensitivity and reproducibility toward probe molecule, the AuNPs@MoS_2-3 nanocomposite had been selected as SERS-active substrate in the following experiment.

To study the SERS performance of AuNPs@MoS_2-3 substrate, the Raman peak located at 1362 cm^{-1} was chosen as the signature to determine the concentration of R6G in the samples. As shown in Figure 5C, SERS spectra of a series of R6G were obtained on AuNPs@MoS_2-3 substrate. The Raman signal of R6G was obviously increased with the concentrations of R6G ranging from 5×10^{-7} M to 10^{-4} M. Due to its stronger coupling ability of AuNPs and MoS_2 nanosheet, the AuNPs@MoS_2 Raman-active substrate can detect as low as 1×10^{-6} M R6G (Figure 5D). For quantification, the enhancement factor ($EF = [(I_{sers}/I_{bulk})(N_{bulk}/N_{sers})]$) was calculated according to the previously reported.[28,29] Figure S5 showed the normal Raman spectrum of 10^{-1} M R6G on silicon wafer and SERS spectrum of 10^{-4} M R6G on AuNPs@MoS_2-3 nanocomposite, respectively. On the basis of the intensity of the carbon skeleton stretching modes at 1362 cm^{-1}, the EF was calculated to be 8.2×10^5, showing the good SERS activity of the substrate.

Uniformity of SERS-active substrate played a vital role in practical applications. An area (15 μm × 13 μm) of the AuNPs@MoS_2-3 substrate was selected for point-by-point SERS mapping, which were recorded with a 2 μm step for R6G on AuNPs@MoS_2-3 substrate (Supporting Information Figure S6). Each spot showed distinctive Raman intensity, revealing the AuNPs@MoS_2-3 substrate had excellent capability to enhance the Raman signals of R6G molecule. The experimental results indicated the AuNPs@MoS_2-3 substrate possess good reproducibility for molecule detection. To further evaluate the reproducibility of SERS signals, the SERS intensity of R6G from the mapping spectra (49 spots) is shown in Figure 6. To get a statistically meaningful result, the relative standard deviation (RSD) of the Raman intensity of R6G was calculated. The RSD of the Raman shifts at 775, 1185, 1311, 1362, 1511, and 1652 cm^{-1} are 24.2%, 26.8%, 24.5%, 20.6%, 20.3%, and 23.1%, respectively, revealing as-prepared AuNPs@MoS_2-3 nanocomposite could be considered as a promising substrate for SERS detection with high reproducibility.[30]

CONCLUSION

In conclusion, an efficient SERS-active substrate has been developed by synthesizing AuNPs@MoS_2 nanocomposite. Under the optimal conditions, uniform and high density of AuNPs has grown in situ on the surface of MoS_2 nanosheet, creating many hot spots to amplify the SERS activity toward

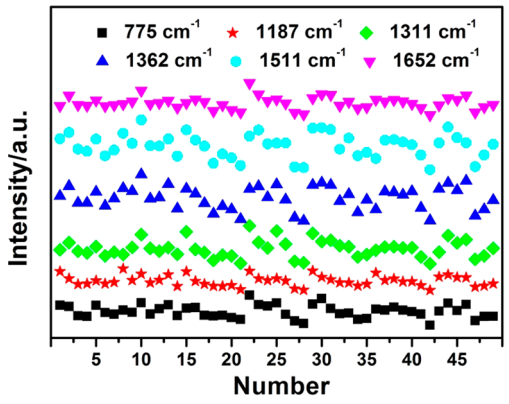

Figure 6. Raman intensities of R6G molecules (49 spots) collected on AuNPs@MoS_2-3 substrate.

the probe molecule. The AuNPs@MoS_2-3 substrate possesses good sensitivity and reproducibility, suggesting that the AuNPs@MoS_2 nanocomposite has great potential in SERS applications of chemical and biological molecules detection.

■ ASSOCIATED CONTENT

Ⓢ Supporting Information

Additional supporting data such as HRTEM image of AuNPs@MoS_2-3 nanocomposite and size distribution histograms of AuNPs@MoS_2-3 nanocomposites, EDX spectra of MoS_2 and AuNPs@MoS_2-3 nanocomposite, Raman spectrum of MoS_2 and AuNPs@MoS_2-3, SERS spectra of R6G molecules on AuNPs and AuNPs@MoS_2-3 nanosheet, normal Raman spectrum of 10^{-1} M R6G on silicon wafer and SERS spectrum of 10^{-4} M R6G on AuNPs@MoS_2-3 nanocomposite, and selected SERS maps of R6G molecules (1311 cm^{-1}, step size 2 μm) on AuNPs@MoS_2-3 substrate. This material is available free of charge via the Internet at http://pubs.acs.org.

■ AUTHOR INFORMATION

Corresponding Authors

*E-mail: chaojie@sinap.ac.cn. Tel: +86 25 85866333.
*E-mail: iamlhwang@njupt.edu.cn. Tel: +86 25 85866333.

Notes

The authors declare no competing financial interest.

■ ACKNOWLEDGMENTS

This work was financially supported by the National Basic Research Program of China (2012CB933301), the National Natural Science Foundation of China (21305070, 21475064, 81273409 and 61302027), the Natural Science Foundation of Jiangsu Province (BK20130861, BK20130871), the Ministry of Education of China (IRT1148, 20123223110007 and 20133223120013), the Scientific Research Foundation of Nanjing University of Posts and Telecommunications (NY212033 and NY212032), and the Priority Academic Program Development of Jiangsu Higher Education Institutions (PAPD). The authors would like to thank Prof. Yao He for fruitful discussion, and Xiangxu Jiang and Yiling Zhong for their technique help.

■ REFERENCES

(1) Wei, X.; Su, S.; Guo, Y.; Jiang, X.; Zhong, Y.; Su, Y.; Fan, C.; Lee, S. T.; He, Y. A Molecular Beacon-Based Signal-Off Surface-Enhanced Raman Scattering Strategy for Highly Sensitive, Reproducible, and Multiplexed DNA Detection. *Small* **2013**, *9* (15), 2493−2499.
(2) Kneipp, J.; Kneipp, H.; Kneipp, K. SERS-a Single-Molecule and Nanoscale Tool for Bioanalytics. *Chem. Soc. Rev.* **2008**, *37* (5), 1052−1060.
(3) Zavaleta, C. L.; Smith, B. R.; Walton, I.; Doering, W.; Davis, G.; Shojaei, B.; Natan, M. J.; Gambhir, S. S. Multiplexed Imaging of Surface Enhanced Raman Scattering Nanotags in Living Mice Using Noninvasive Raman Spectroscopy. *Proc. Natl. Acad. Sci. U.S.A.* **2009**, *106* (32), 13511−13516.
(4) An, Q.; Zhang, P.; Li, J.-M.; Ma, W.-F.; Guo, J.; Hu, J.; Wang, C.-C. Silver-Coated Magnetite-Carbon Core-Shell Microspheres as Substrate-Enhanced SERS Probes for Detection of Trace Persistent Organic Pollutants. *Nanoscale* **2012**, *4* (16), 5210−5216.
(5) Qian, X. M.; Nie, S. M. Single-Molecule and Single-Nanoparticle SERS: From Fundamental Mechanisms to Biomedical Applications. *Chem. Soc. Rev.* **2008**, *37* (5), 912−920.
(6) Wustholz, K. L.; Henry, A.-I.; McMahon, J. M.; Freeman, R. G.; Valley, N.; Piotti, M. E.; Natan, M. J.; Schatz, G. C.; Duyne, R. P. V. Structure-Activity Relationships in Gold Nanoparticle Dimers and Trimers for Surface-Enhanced Raman Spectroscopy. *J. Am. Chem. Soc.* **2010**, *132* (31), 10903−10910.
(7) Braun, G.; Lee, S. J.; Dante, M.; Nguyen, T.-Q.; Moskovits, M.; Reich, N. Surface-Enhanced Raman Spectroscopy for DNA Detection by Nanoparticle Assembly onto Smooth Metal Films. *J. Am. Chem. Soc.* **2007**, *129* (20), 6378−6379.
(8) Jiang, Z.; Jiang, X.; Su, S.; Wei, X.; Lee, S.; He, Y. Silicon-Based Reproducible and Active Surface-Enhanced Raman Scattering Substrates for Sensitive, Specific, and Multiplex DNA Detection. *Appl. Phys. Lett.* **2012**, *100* (20), 203104.
(9) Ling, X.; Fang, W.; Lee, Y.-H.; Araujo, P. T.; Zhang, X.; Rodriguez-Nieva, J. F.; Lin, Y.; Zhang, J.; Kong, J.; Dresselhaus, M. S. Raman Enhancement Effect on Two-Dimensional Layered Materials: Graphene, H-BN and MoS_2. *Nano Lett.* **2014**, *14*, 3033−3040.
(10) Zhao, J.; Zhang, Z.; Yang, S.; Zheng, H.; Li, Y. Facile Synthesis of MoS_2 Nanosheet-Silver Nanoparticles Composite for Surface Enhanced Raman Scattering and Electrochemical Activity. *J. Alloys Compd.* **2013**, *559*, 87−91.
(11) Sun, L.; Hu, H.; Zhan, D.; Yan, J.; Liu, L.; Teguh, J. S.; Yeow, E. K. L.; Lee, P. S.; Shen, Z. Plasma Modified MoS_2 Nanoflakes for Surface Enhanced Raman Scattering. *Small* **2014**, *10* (6), 1090−1095.
(12) Li, H.; Wu, J.; Yin, Z.; Zhang, H. Preparation and Applications of Mechanically Exfoliated Single-Layer and Multilayer MoS_2 and WSe_2 Nanosheets. *Acc. Chem. Res.* **2014**, *47* (4), 1067−1075.
(13) Bang, G. S.; Nam, K. W.; Kim, J. Y.; Shin, J.; Choi, J. W.; Choi, S.-Y. Effective Liquid-Phase Exfoliation and Sodium Ion Battery Application of MoS_2 Nanosheets. *ACS Appl. Mater. Interfaces* **2014**, *6* (10), 7084−7089.
(14) Ganatra, R.; Zhang, Q. Few-Layer MoS_2: A Promising Layered Semiconductor. *ACS Nano* **2014**, *8* (5), 4074−4099.
(15) Huang, X.; Zeng, Z.; Bao, S.; Wang, M.; Qi, X.; Fan, Z.; Zhang, H. Solution-Phase Epitaxial Growth of Noble Metal Nanostructures on Dispersible Single-Layer Molybdenum Disulfide Nanosheets. *Nat. Commun.* **2013**, *4*, 1444.
(16) Shi, Y.; Huang, J.-K.; Jin, L.; Hsu, Y.-T.; Yu, S. F.; Li, L.-J.; Yang, H. Y. Selective Decoration of Au Nanoparticles on Monolayer MoS_2 Single Crystals. *Sci. Rep.* **2013**, *3*, 1839.
(17) Kim, J.; Byun, S.; Smith, A. J.; Yu, J.; Huang, J. Enhanced Electrocatalytic Properties of Transition-Metal Dichalcogenides Sheets by Spontaneous Gold Nanoparticle Decoration. *J. Phys. Chem. Lett.* **2013**, *4* (8), 1227−1232.
(18) Yuwen, L.; Xu, F.; Xue, B.; Luo, Z.; Zhang, Q.; Bao, B.; Su, S.; Weng, L.; Huang, W.; Wang, L.-H. General Synthesis of Noble Metal (Au, Ag, Pd, Pt) Nanocrystals Modified MoS_2 Nanosheets and Enhanced Catalytic Activity of Pd-MoS_2 for Methanol Oxidation. *Nanoscale* **2014**, *6*, 5762−5769.
(19) Su, S.; Sun, H.; Xu, F.; Yuwen, L.; Fan, C.; Wang, L. Direct Electrochemistry of Glucose Oxidase and a Biosensor for Glucose Based on a Glass Carbon Electrode Modified with MoS_2 Nanosheets

Decorated with Gold Nanoparticles. *Microchim. Acta* **2014**, *181*, 1497−1503.
(20) Sreeprasad, T.; Nguyen, P.; Kim, N.; Berry, V. Controlled, Defect-Guided, Metal-Nanoparticle Incorporation onto MoS_2 via Chemical and Microwave Routes: Electrical, Thermal, and Structural Properties. *Nano Lett.* **2013**, *13* (9), 4434−4441.
(21) Joensen, P.; Frindt, R.; Morrison, S. R. Single-Layer MoS_2. *Mater. Res. Bull.* **1986**, *21* (4), 457−461.
(22) Chou, S. S.; De, M.; Kim, J.; Byun, S.; Dykstra, C.; Yu, J.; Huang, J.; Dravid, V. P. Ligand Conjugation of Chemically Exfoliated MoS_2. *J. Am. Chem. Soc.* **2013**, *135* (12), 4584−4587.
(23) Coleman, J. N.; Lotya, M.; O'Neill, A.; Bergin, S. D.; King, P. J.; Khan, U.; Young, K.; Gaucher, A.; De, S.; Smith, R. J.; Shvets, I. V.; Arora, S. K.; Stanton, G.; Kim, H.-Y.; Lee, K.; Kim, G. T.; Duesberg, G. S.; Hallam, T.; Boland, J. J.; Wang, J. J.; Donegan, J. F.; Grunlan, J. C.; Moriarty, G.; Shmeliov, A.; Nicholls, R. J.; Perkins, J. M.; Grieveson, E. M.; Theuwissen, K.; McComb, D. W.; Nellist, P. D.; Nicolosi, V. Two-Dimensional Nanosheets Produced by Liquid Exfoliation of Layered Materials. *Science* **2011**, *331* (6017), 568−571.
(24) Jana, N. R.; Gearheart, L.; Murphy, C. J. Seeding Growth for Size Control of 5−40 nm Diameter Gold Nanoparticles. *Langmuir* **2001**, *17* (22), 6782−6786.
(25) Michaels, A. M.; Nirmal, M.; Brus, L. Surface Enhanced Raman Spectroscopy of Individual Rhodamine 6G Molecules on Large Ag Nanocrystals. *J. Am. Chem. Soc.* **1999**, *121* (43), 9932−9939.
(26) Nie, S.; Emory, S. R. Probing Single Molecules and Single Nanoparticles by Surface-Enhanced Raman Scattering. *Science* **1997**, *275* (5303), 1102−1106.
(27) Liu, Y.-T.; Duan, Z.-Q.; Xie, X.-M.; Ye, X.-Y. A Universal Strategy for the Hierarchical Assembly of Functional 0/2D Nano-hybrids. *Chem. Commun.* **2013**, *49* (16), 1642−1644.
(28) He, Y.; Su, S.; Xu, T.; Zhong, Y.; Zapien, J. A.; Li, J.; Fan, C.; Lee, S.-T. Silicon Nanowires-Based Highly-Efficient SERS-Active Platform for Ultrasensitive DNA Detection. *Nano Today* **2011**, *6* (2), 122−130.
(29) Chang, C.-C.; Yang, K.-H.; Liu, Y.-C.; Hsu, T.-C.; Mai, F.-D. Surface-Enhanced Raman Scattering-Active Au/SiO_2 Nanocomposites Prepared Using Sonoelectrochemical Pulse Deposition Methods. *ACS Appl. Mater. Interfaces* **2012**, *4* (9), 4700−4707.
(30) Que, R.; Shao, M.; Zhuo, S.; Wen, C.; Wang, S.; Lee, S. T. Highly Reproducible Surface-Enhanced Raman Scattering on a Capillarity-Assisted Gold Nanoparticle Assembly. *Adv. Funct. Mater.* **2011**, *21* (17), 3337−3343.